

An Efficient Model for Predicting the Segregation Profile of Binary Fluidized Beds

Mohamed Sobhi Al-Agha^{1,2}, Pál Szentannai^{2*}

¹ Department of Mechanical Engineering, Faculty of Engineering, Kafrelsheikh University, 33516 Kafrelsheikh, El-Giesh Street 5, Egypt

² Department of Energy Engineering, Faculty of Mechanical Engineering, Budapest University of Technology and Economics, 1111 Budapest, Muegyetem rkp. 9, Hungary

* Corresponding author, e-mail: szentannai@energia.bme.hu

Received: 25 January 2018, Accepted: 07 June 2018, Published online: 10 July 2018

Abstract

In most cases, the stationary fluidized beds are composed of two different particle classes (inert and active particles), and the concentration profile of these binary beds along the vertical axis is crucial regarding the effectiveness of the reactor. The present study introduces a semi-empirical 1D mathematical model for predicting the vertical concentration profile of binary fluidized beds. The proposed model is a developed and applicable version of the so-called Gibilaro and Rowe two-phase model, in which the differential equations describing the jetsam movement in the bulk and wake phases were solved numerically. The main work was to determine the parameters of the basic model, which was carried out by means of an advanced multi-step parameter fitting procedure. A more general form was established, which is based on direct linkage with the operating parameters that can be directly set and measured on the system. Comparisons with very diverse measured data sets available in the literature prove the accuracy of this model. Additional comparisons pointed out that the realization of this model is numerically inexpensive as it is several orders of magnitude faster than the available 2D and 3D models.

Keywords

two-phase model, G-R model, semi-empirical 1D model, mixing and segregation, fluidized bed conversion

1 Introduction

The significance of fluidized bed reactors is in their ability to assure an intensive contact between solid and gaseous reactants. Catalytic cracking is one traditional application area, and the energy industry shows a rapid growth in its applications as fluidized bed combustors, *gasifiers*, and many other environment-friendly conversion technologies [1, 2].

In fluidized bed reactors, binary beds are applied in most cases, that is, the bed is a mixture of two different particle classes, the inert and the active particles. The phenomenon of mixing and segregation of binary fluidized beds has a great impact on the operation and characteristics of these reactors. It controls bed uniformity and internal reaction kinetics, heat transfer and ash composition of industrial and power generation applications in many fluidized beds.

Scientific researches on the co-fluidization of two different types of solid particles began several decades ago, and one of the first determining results belong to Nienow et al. [3]. They introduced the terms *flotsam* and *jetsam*

referring to the particles tending to float to the bed surface and sink to the bottom, respectively. Experimental researches on mixing and segregation have been carried out on various systems of granular mixtures of different densities and/or sizes [3–8]. Also, fluidization velocity has been found to be a significant parameter of the mixing phenomenon [9–14], as well as of the fluidization procedure [15, 16]. But, the experimental pilot scale test-rigs encountered difficulties when extended to industrial scale reactors [17, 18].

Therefore, theoretical model developments, in parallel with experiments, can help to improve our knowledge about these exciting mechanical systems.

In general, the computational models used in simulation of fluidized beds can be classified according to their geometric complexity into 1D, 2D, and 3D models. In the past decade the fast development of computational facilities had a great influence on upgrading the simulation models from 1D to 2D and 3D models. Actually, modeling the mixing

and segregation phenomenon of binary beds by means of commercial 3D codes is possible. However, the correct selection of the appropriate submodels and parameters for any specific cases is still a big challenge (see e.g. [19–23]), and each individually calculated result requires validation. This fact, together with the computational expensive character of these models is a strong motivation for developing numerically simple and effective mathematical models.

Improvements in theoretical 1D modeling have been carried out to explore mixture composition at different zones within the bed, and simulate the hydrodynamic interaction between fluidization bubbles and the particulate material. In this way, two differential equations based on the two-phase theory [24] to describe the movement of jetsam bulk and wake phases in binary mixtures have been formulated by Gibilaro and Rowe (G–R, [25]) as follows:

$$\beta \frac{\partial^2 C_B}{\partial Z^2} + (\lambda + 1 - 2C_B) \frac{\partial C_B}{\partial Z} + \gamma \lambda (C_W - C_B) = 0, \quad (1)$$

$$\lambda \frac{\partial C_B}{\partial Z} + \gamma \lambda (C_B - C_W) = 0, \quad (2)$$

where C_B and C_W stand for jetsam concentration in the bulk and wake phases along the axial direction, Z , and β , γ , and λ are analytical parameters expressing axial mixing / segregation, phase exchange / circulation and circulation / segregation. This set of equations form the basis for many subsequent researches followed also by the current one, hence they will be discussed thoroughly in the following sections of this paper.

Three different experimental "cases" (i.e. strong mixing, strong segregation and partial segregation) were selected in the original publication, which could be solved analytically [25]. In each of them one of the mechanisms responsible for the mixing and segregation phenomena was neglected. A brief overview of these "cases" were also given in a paper introducing an earlier, more specific result of the current model development [26].

For example "case 2", which took all mechanisms, except axial dispersion, into account, was applied on many theoretical studies [11, 12, 27]; however, according to other authors, axial dispersion influence was very significant and not negligible [10]. Garcia-Ochoa et al. [10] used only cases 1 and 3, and they achieved good validation for the binary mixtures of different densities and identical size. However, it was unclear how these analytical parameters obtained modified to give reasonable accuracy for other different mixture cases. Naimer et al. [27] developed a method for

setting up a linkage between the analytical parameters and the direct operating variables (like gas velocity, densities, etc.). In this way, the G–R model could be easily adapted to different flow patterns with different operating conditions. They used the G–R analytical solution disregarding axial mixing in the bulk phase. A limited accuracy of the model was found at high overall jetsam concentrations.

As an alternative approach, stochastic 1D modeling of binary mixtures was also developed by some researchers [28], but Hoffmann et al. [12] reported that the G–R model was the best theoretical 1D model for predicting the mixing and segregation behaviour of all classes of binary mixtures.

For slugging pattern fluidized beds, a modified set of coefficients of the G–R model was also proposed [29]. Leaper et al. [13] carried out a numerical solution of the G–R equations taking into account the effect of all mixing / segregation mechanisms with further evaluation of the solution by setting a model coefficient to some non-physical values to compare with experimental data. It was noticed that there was deviation between their model predictions, and the experimental test cases at low fluidization velocities. But, the full solution of the G–R model is still not applicable because of the absence of a generally valid linkage with the direct operating variables, such as fluidization velocity, particle sizes, and densities, etc.

The objective of the present study is to develop an overall semi-empirical model that is (i) numerically inexpensive, (ii) accurate, at least as other models, and (iii) relies on direct operating variables.

The approach to be discussed here considers all mechanisms of the general G–R model, which will be calibrated by using all available experimental test cases found in the literature. They cover a broad range of different densities, total jetsam mass ratios, as well as fluidization velocities. (This broad case coverage was an important goal of the current semi-empirical model development, while no specific structural target was formulated like focusing on detailed mechanism descriptions, e.g.) A new set of functions will be formulated to supply the G–R coefficients as functions of the selected direct operating parameters. Verification of the resulting overall model will be carried out not by comparing the fitting and fitted data, but by comparing the vertical segregation profiles measured and calculated on the same set of known experiments. This proofing method is followed by all authors of the known specific models in order to rely the model on the biggest possible number of experimental data [10–13, 27, 30].

2 Overall optimization of the Gibilaro–Rowe model

The general G–R model of binary fluidized beds, which is given by Eqs. (1) and (2), and which is used in the present study, was constructed based on the two-phase theory of Toomey and Johnstone [24]. The jetsam transport in the binary bed is mainly caused by four different mechanisms (see Fig. 1) outlined briefly as follows.

1. *Axial mixing* is the part of bubbles action that makes the jetsam particles move upward in a pseudo-diffusion manner.
2. *Segregation* is the reaction of jetsam particles in the bulk phase to refill the volume of the displaced bubble more rapidly than the flotsam solids.
3. *Circulation* is the action of the wake-phase jetsam particles carried up to the top of the bed by the bubbles when they leave the bubble and join the bulk phase flowing downward.
4. *Exchange* is the mechanism representing the transport of jetsam particles between the bulk and wake phases due to continuous feeding and shedding particles from the bulk to the bubbles, respectively.

The model assumptions are as follows:

- The space occupied by the bubbles is ignored.
- The volumetric flow rate of solids is constant along all horizontal planes through the bed.
- The amount of segregation occurring at any point is proportional to the jetsam concentration at that point.

The two model Eqs. (1) and (2) are the conservation laws of jetsam formulated for both bulk and wake phases considering four basic mechanisms as summarized on Fig. 1.

The full model also requires two further algebraic equations describing the average volume and mass concentration of jetsam, respectively, as follows:

$$C_{ave} = (1 - f_w)C_B + f_w C_W \quad (3)$$

$$X_{ave} = \frac{C_{ave} \left(\frac{\rho_j}{\rho_f} \right)}{1 - \left(1 - \frac{\rho_j}{\rho_f} \right) C_{ave}} \quad (4)$$

where f_w is the volumetric fraction of all solids in the wake phase, as discussed in the original publication [25]. Equations (3) and (4) are in fact just for post-processing of the solution of Eqs. (1) and (2). An overview of the

mechanisms responsible for the mixing and segregation phenomena is given in Fig. 1.

Besides the analytical solutions, authors were working on finding a full numerical solution of the G–R model equations. According to our knowledge, no overall solution with generally valid model parameters was reported to date. Therefore, we started to solve the model equations (full solution) by using the 4th order Runge-Kutta method [31]. Then, the empirical correlations of coefficients from literature [11, 12, 27, 32, 33] were applied, all of them based on bubble action inside the fluidized bed. The results showed good agreement in some cases, while giving poor predictions for some others. This may be due to the limited range of these correlations.

Thus, in our present procedure the proposed way is calibrating the numerical model with pure experimental test cases for a full, overall, and easy-to-handle solution. This procedure will be introduced step by step in the following subsections.

2.1 Choosing experimental variables as model inputs

The G–R model has four independent coefficients, β , λ , f_w , and γ (see Eqs. (1)–(4)). Thus, it requires four correlations to estimate those coefficients. Fortunately, here there is good knowledge about the physical variables controlling the phenomena, and they can be chosen as model inputs. They are excess fluidization-velocity ratio $(u - u_{mf})/u_{mf}$, overall jetsam mass fraction x_j , particle-size ratio d_j/d_f , and particle-density ratio ρ_j/ρ_f . Some further parameters do definitely influence the

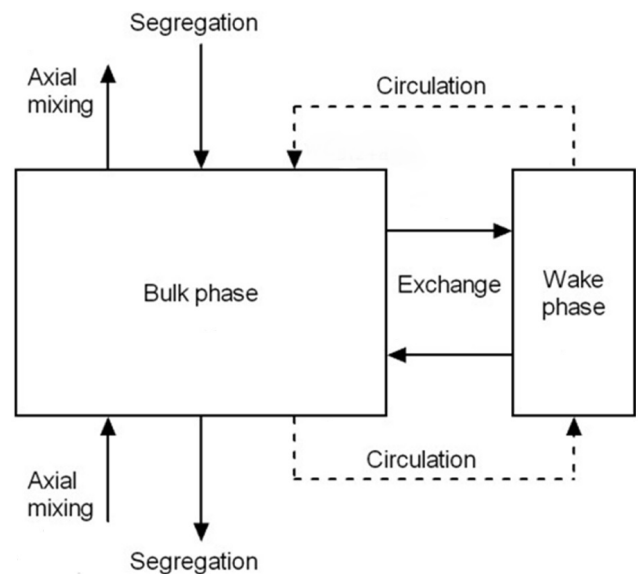


Fig. 1 Conservation elements and mass transport mechanisms considered in the G–R model [25]

mixing / segregation process such as bed geometrical aspect ratio (height / diameter) [11, 30]. In the current model the above listed ones are considered, however, further researches are welcome to improve the model by also including other influencing parameters.

It is, of course, still not visible here whether this set of physical parameters will be enough for a full description of the actual mixing / segregation profile of the fluidized bed. A final verification of the resulting model will answer this question.

2.2 Selecting published measurement data sets

The numerical model has to be calibrated with different experimental data in order to get the proper coefficients, and so to make the model valid over a wide range of operating conditions. Published data will be used in order to assure versatility in the parameter values. As the calibration should be based on the direct operating variables listed in the previous subsection, an evident criterion is their availability in the publication. This did not seem obvious for only one parameter, the minimum fluidization velocity u_{mf} of the mixture, which can be calculated from those of the components as follows [27]:

$$u_{mf} = u_s + \left(\frac{u_B}{u_s} \right)^{x_B^2} \quad (5)$$

Here u_s and u_B are the minimum fluidization velocities of the smaller and bigger components, respectively, and x_B stands for the total mass fraction of the bigger (jetsam or flotsam) particles. As these data are missing from many publications, they had to be excluded from the calibration. (Note that estimating the absent minimum fluidization velocities u_s and u_B based on other data could be possible by means of some available correlations. However, the high inaccuracies of these correlations ranging from -94 % to +98 % make this approach fully unacceptable for generating values to be applied as basis for parameter fitting.)

In spite of these strict but evident criteria, we succeeded to find 14 experimental data sets in four independent publications [10, 13, 27, 30] covering a rather broad range of input variables, as summarized in columns B to E of Table 1.

2.3 Specific parameter fitting

Finding the best fitting G–R model parameters to each individual experimental segregation profile is possible. It was done by us considering the full G–R model without the exclusion of any phenomena, and the results are summarized in columns F to I in Table 1.

This is to mention that these results give good models, but for the actual cases only, hence they are specific models without considering the influences of the direct operating parameters (fluidization velocity, etc.). This is

Table 1 Experimental data sets found and applied for calibrating the overall model. Columns F – I: results of the parameter fitting procedure.

A	B				C			
	Experimental conditions				Best fit model parameters			
Experiment ID, Ref.	mass fraction x_j	density ratio ρ_j / ρ_f	particle-size ratio d_j / d_f	fluidization velocity ratio u / u_{mf}	β	λ	f_w	γ
N1 [27]	0.100	8860/2950	273/461	0.336/0.195	0.012	0.001	0.001	0.050
J1 [30]	0.200	2476/1064	231/231	0.059/0.044	0.0085	0.040	0.050	0.950
J2 [30]	0.250	2476/1064	116/275	0.036/0.019	0.012	0.060	0.035	0.850
J3 [30]	0.250	2476/2476	231/116	0.062/0.034	0.062	0.007	1.150	0.110
N2 [27]	0.400	8860/2950	273/461	0.337/0.196	0.020	0.052	0.005	0.750
N3 [27]	0.400	8860/2950	273/461	0.650/0.196	0.015	0.075	0.125	0.850
HR1 [11]	0.500	8650/2490	273/281	0.312/0.085	0.015	0.200	0.280	0.950
HR2 [11]	0.500	11320/2490	112/281	0.146/0.068	0.012	0.195	0.005	0.400
HF1 [12]	0.500	8750/2510	235/565	0.290/0.210	0.016	0.130	0.005	0.500
HF2 [12]	0.750	8750/2510	235/565	0.525/0.239	0.010	0.090	0.410	0.900
J4 [30]	0.690	2476/1064	116/275	0.045/0.026	0.010	0.380	0.140	0.200
N4 [27]	0.700	8860/2950	273/461	0.336/0.199	0.055	0.008	0.075	0.950
J5 [30]	0.750	2476/2476	231/116	0.042/0.019	0.012	0.180	0.700	0.050
J6 [30]	0.750	2476/1064	231/231	0.078/0.030	0.0115	0.620	0.070	0.300

the point that most known reports arrived to by now, and this is the shortage the current work intended to fill up by elaborating an overall model.

2.4 Buckingham PI fitting

The core idea of finding a suitable linkage between the G–R coefficients and experimental conditions depends on the direct operating parameters impacting the phenomena. As described in the previous sections, there are some variables having a clear influence on the mixing and segregation phenomena such as density ratio, particle-sized ratio, total jetsam mass fraction, and fluidization velocity [5, 33–35].

The Buckingham PI-theorem [36] was used for finding the model correlations describing the influences of the above mentioned direct operating variables, which were selected as the PI input variables [37]:

$$\pi_1 = x_j, \pi_2 = \frac{\rho_j}{\rho_f}, \pi_3 = \frac{d_j}{d_f}, \pi_4 = \frac{u - u_{mf}}{u_{mf}}.$$

Every dimensionless parameter was plotted and fitted independently with the G–R model coefficients found and listed in columns F to I of Table 1. For example, the curve-fitting results of the coefficient β were obtained as follows:

$$\beta^{-1}(\pi_1) = f_{\beta,1} \left(e^{-2.404x_j} \right), \beta^{-1}(\pi_2) = f_{\beta,2} \left(\left(\frac{\rho_j}{\rho_f} \right)^{-0.471} \right),$$

$$\beta^{-1}(\pi_3) = f_{\beta,3} \left(e^{0.5 \frac{d_j}{d_f}} \right), \beta^{-1}(\pi_4) = f_{\beta,4} \left(e^{0.1404 \frac{u - u_{mf}}{u_{mf}}} \right).$$

After that, the superposition method was applied to get the final, general correlation of the model coefficient as a function of those dimensionless groups as follows:

$$\beta^{-1}(\pi_1, \pi_2, \pi_3, \pi_4) = f_{\beta} \left(e^{-2.404x_j} \left(\frac{\rho_j}{\rho_f} \right)^{-0.471} e^{0.5 \frac{d_j}{d_f}} e^{0.1404 \frac{u - u_{mf}}{u_{mf}}} \right). \quad (6)$$

To find these final f functions for each G–R model parameters ($f_{\beta}, f_{\lambda}, f_{f_w},$ and f_{γ}), a next fitting procedure is required. In this study, not just the best fitting values were used for this next fitting step, but also some others, the quality of which were also close to the optimum, as discussed in the next subsection.

2.5 Setting up the final form of the overall model

Instead of using one optimum-solution point in this curve-fitting process, all solutions with the minimum standard deviation below 2 % were applied, as this led to a considerable improvement in the fitting process and the final model. Fig. 2 shows the solution contours at different values of the G–R model coefficients on the example of system HF1 (see Table 1).

It is clear from the figure that the solution converges within the dark blue area as it refers to the minimum absolute-error zones below 2 %. Those optimum-solution points will be used in the next fitting step, henceforth. Similarly, this procedure was applied for all experimental systems listed in Table 1.

Fig. 3 shows the values obtained this way on the fitting charts of the G–R coefficients as functions of binary fluidized bed operating conditions, together with the best fitting lines and their equations. Note that the regression factor, R^2 cannot be used here as a precise measure of this data fitting step because the basis of this fitting was not the set of the best points, but multiple solution points (a "solution cloud"), as shown in Fig. 2.

The final overall model summary representation can be found in Table 2. Besides including the physical variables based calculation of the G–R model parameters, this table also refers to the basic equations and the initial boundary conditions proposed and used by us throughout the model verification to be discussed in the next section. As boundary conditions, it was assumed that the bottom layer is totally bulk, and this status changes very slowly in space (i.e., no jetsam solids are located in the bubbles, $C_B|_{z=0} = 1, C_w|_{z=0} = 0, \frac{\partial C_B}{\partial Z}|_{z=0} = 0$). This assumption arises from the fact that the bubble sizes are very small at this level, close to the nozzles.

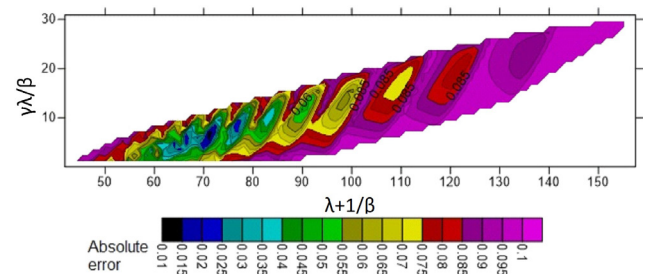


Fig. 2 Standard deviation contours of different solutions of the G–R model in comparison with experimental data – as an example for case HF1 in Table 1.

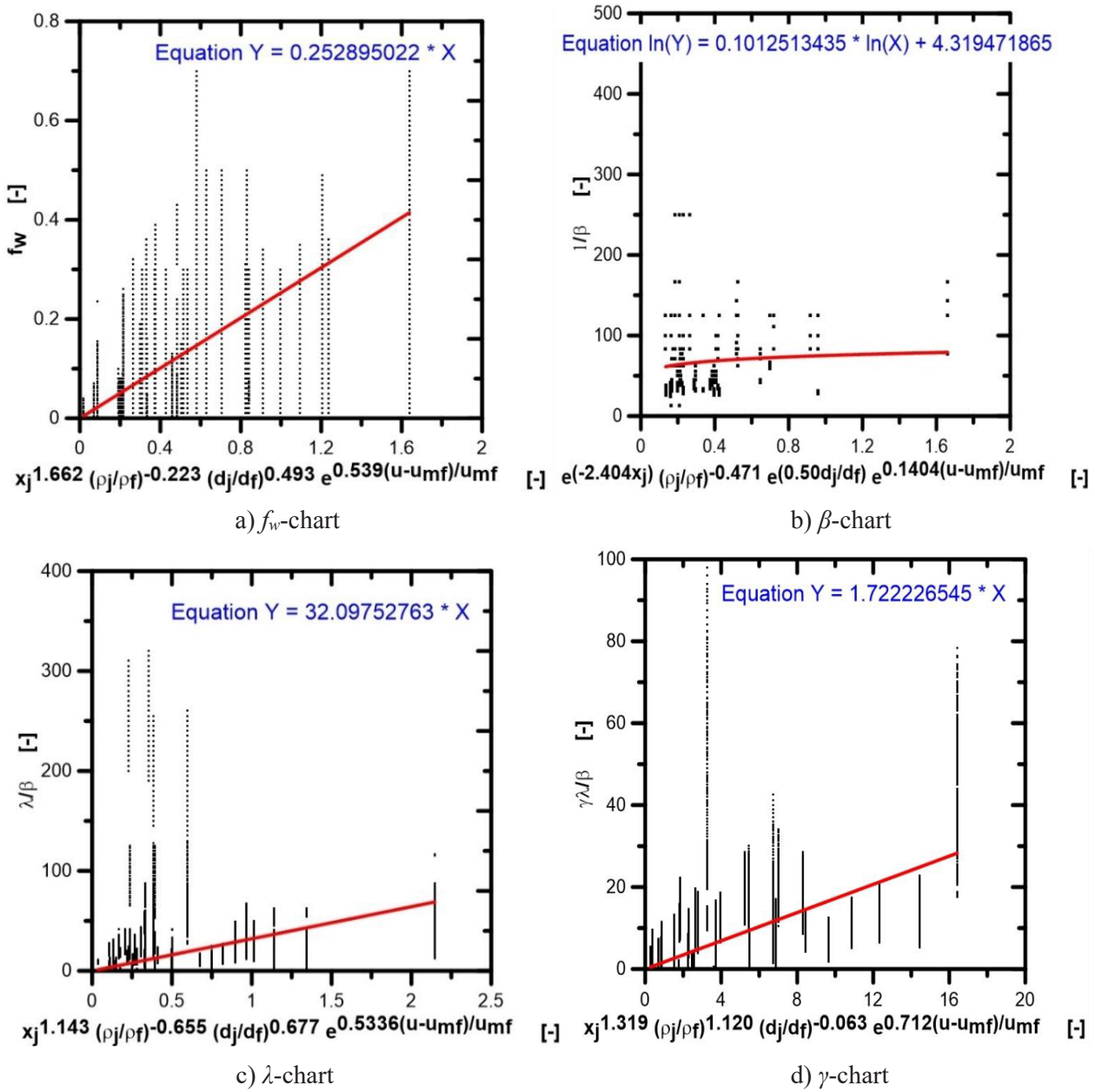


Fig. 3 Charts of the G–R model coefficients and fitting results

3 Discussion

3.1 Comparison with previous 1D models

The overall model was tested with all the available, measured data sets. The results of the proposed semi-empirical 1D model are discussed here and compared with the predictions of the previous theoretical 1D models. Some representative cases can be seen in Fig. 4. As visible, the proposed model assures an overall acceptable agreement with the experimental results.

Subfigure N1 represents strong segregation behavior, the only model which predicts this trend properly is the proposed

one (see the red solid line), while the other models even fail to give the correct height of the segregation layer. Subfigures N2 and N3 show partial segregating profiles, and, it can clearly be noticed that the current model has better agreement with the experimental data points. Strong mixing systems were represented by subfigures J1, J3, J5, and J6, and it is obviously visible that there is a good agreement between the present 1D model results and the experimental data in most of those systems, while very poor prediction of many other models can be noticed. Subfigures N4, HR2, and J4 indicated poor predictions of the previous theoretical models

Table 2 The proposed overall model summarized

Basic model equations:	
Differential equations to be solved numerically: Eq. (1) and Eq. (2) in this study	Post processing equations: Eq. (3) and Eq. (4) in this study
Coefficients of the above equations as functions of the actual direct operating parameters:	
$f_w = 0.25289 X_{f_w}$	$X_{f_w} = x_j^{1.662} \left(\frac{\rho_j}{\rho_f} \right)^{-0.223} \left(\frac{d_j}{d_f} \right)^{0.493} e^{0.539 \left(\frac{u-u_{mf}}{u_{mf}} \right)}$
$\beta = 0.01331 X_\beta^{-0.10125}$	$X_\beta = e^{-2.404 x_j} \left(\frac{\rho_j}{\rho_f} \right)^{-0.471} e^{0.5 \left(\frac{d_j}{d_f} \right)} e^{0.140 \left(\frac{u-u_{mf}}{u_{mf}} \right)}$
$\lambda = \beta (32.09753 X_\lambda)$	$X_\lambda = x_j^{1.143} \left(\frac{\rho_j}{\rho_f} \right)^{-0.655} \left(\frac{d_j}{d_f} \right)^{0.677} e^{0.534 \left(\frac{u-u_{mf}}{u_{mf}} \right)}$
$\gamma = \frac{\beta (1.72223 X_\gamma)}{\lambda}$	$X_\gamma = x_j^{1.319} \left(\frac{\rho_j}{\rho_f} \right)^{1.120} \left(\frac{d_j}{d_f} \right)^{-0.063} e^{0.712 \left(\frac{u-u_{mf}}{u_{mf}} \right)}$
Initial boundary conditions:	
$C_B _{z=0} = 1, \quad C_W _{z=0} = 0$	$\frac{\partial C_B}{\partial z} \Big _{z=0} = 0$

where they indicate unrealistic profiles of jetsam, although the current model shows a similar partial segregation trend.

The drawback of the present model at high jetsam concentrations can be attributed to the fewer representative experimental cases of higher total jetsam mass fraction ($x_j > 50\%$) in the calibration procedure.

The validity area of empirical and even semi-empirical models cannot be drawn based on the validity areas of the laws of nature built in. Accordingly, also the validity area of the current model can only be judged by the experimental cases appear to be well-modeled. So, the range of validity of the current model can be declared within the following intervals, density ratio: 1.00 – 4.55, particles-size ratio: 0.40 – 2.00, fluidization velocity ratio: 1.34 – 3.67. Figs. 4 and 5 are the basis for this as well.

A summary of absolute error comparison between the present model and the previous models is summarized in Fig. 5, which shows lower error level of the current model compared to the others in almost all cases.

As a further model validation tool, some further experimental data, which were not used in the model fitting procedure, were found [10] and tested, as shown in Fig. 6. They are binary mixtures of Alumina-Polyethylene (System I) and Glass-Alumina (System II), the main data of which are summarized in Table 3. It is visible on Fig. 6 that the present model gives acceptable agreement with experimental data also for the binary systems not included

in the fitting procedure. Of course, a similar comparison could be done with a higher number of experimental data. However, because of the very limited number of available data sets, this method would decrease the number of data sets available for model fitting. In return, it would bring down the quality of the resulted model offered for the scientific community. Large amount of further experimental data are therefore welcome, on the basis of which, the present method could be polished further.

3.2 Comparison with 2D and 3D models

2D and 3D simulations were carried out by using an Eulerian-Eulerian multi-fluid model, which was successfully used in binary fluidized bed simulations [38–40]. Both gas and solid phases were treated as continuum, and modeled by solving the fluid flow governing equations (continuity and momentum) using a commercial code (Ansys Fluent R18.0). The kinetic theory of granular flow was used to calculate granular stresses in the solids momentum equations by solving the granular temperature transport equation [41].

The interaction between the phases were expressed by gas-solid and solid-solid momentum exchange terms in the momentum equations of the phase as in the Fluent theory guide [41]. The gas-solids momentum exchange is greatly dominated by the drag force. In the present study, the Gidaspow drag model was applied as the most commonly used one [42]. For the solid-solid momentum exchange, the

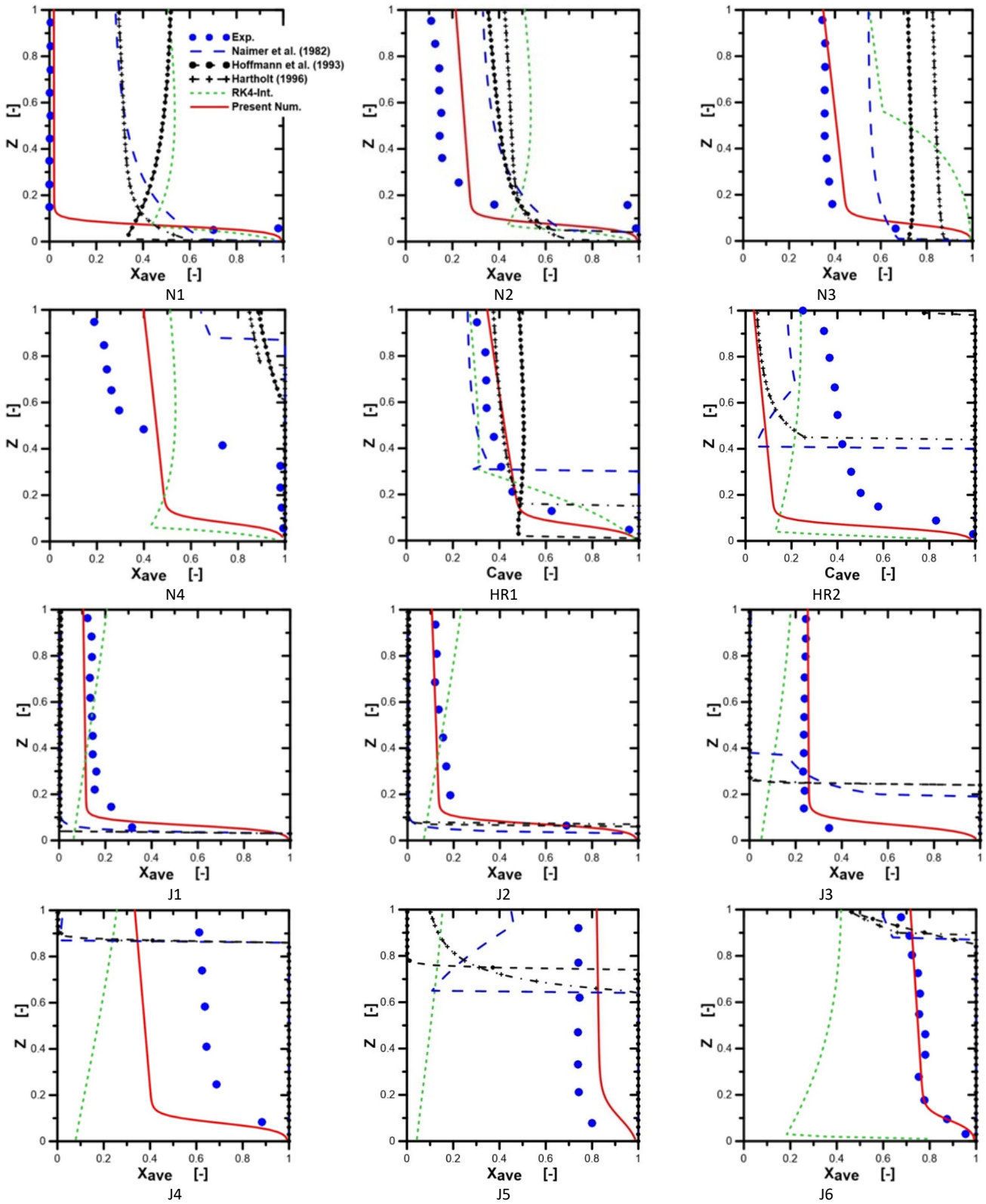


Fig. 4 Comparison between the measured data points (blue symbols), the prediction of the current model (red solid lines), and previous models (broken lines). (The subfigure captions refer to the experiment IDs in column A of Table 1.)

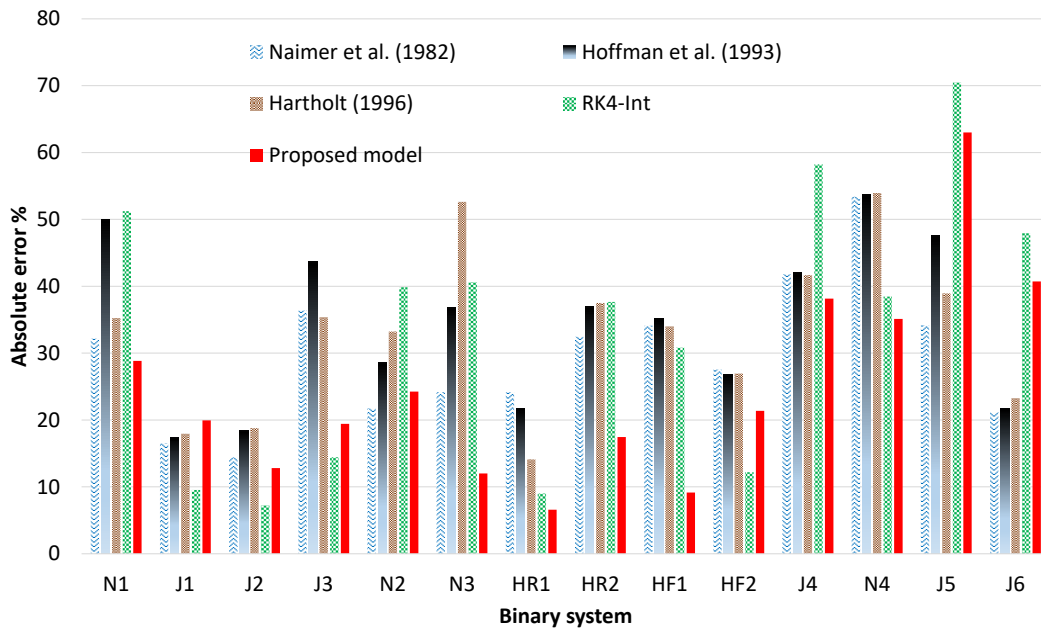


Fig. 5 Comparison summary of the errors of the present model (filled red bars) and previous models (patterned bars of other colors). (The experiment identifiers below the horizontal axis refer to column A in Table 1.)

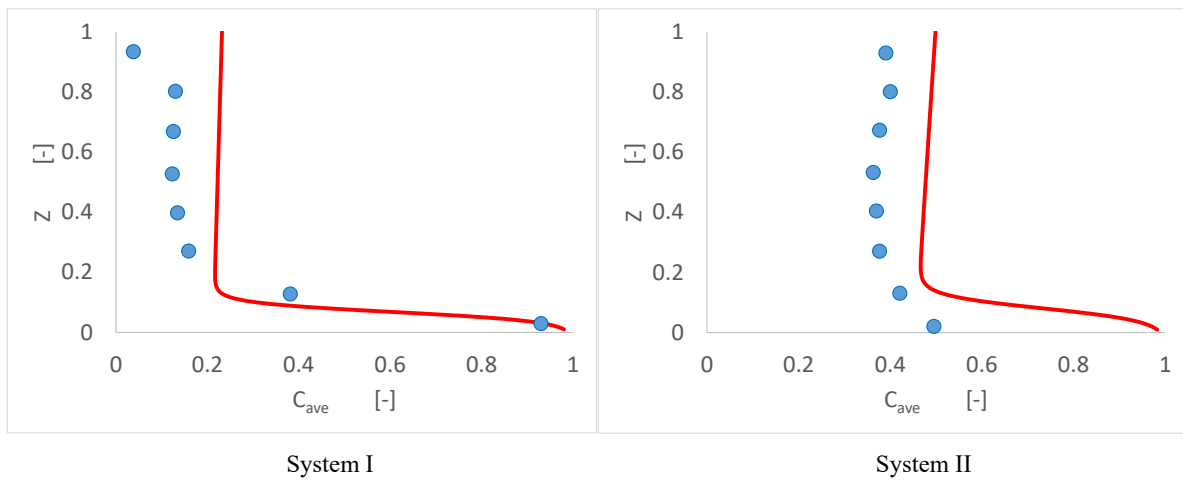


Fig. 6 Comparison between the measured data points of systems not included into the data fitting procedure (blue symbols), and the prediction of the current 1D model (red solid line). The subfigure captions refer to the experiment case IDs of Table 3.)

Syamlal-O'brien symmetric model [43] was applied. This is one of the built-in models recommended for such dense fluidized bed systems. The other computational settings are listed in Table 4.

Table 3 Properties of binary systems not included into the parameter fitting procedure but used for verification

Experiment case ID	x_j	ρ_j / ρ_f	d_j / d_f	u / u_{mf}
System I	0.25	1400/920	4.0/4.0	1.38/0.51
System II	0.50	2200/1400	4.0/4.0	1.68/0.65

Four experimental results from among the list of Table 1 were compared also in this way; N1, N2, N3, and N4. The concentration profiles are shown in Fig. 7 as the example of N1 and N2, while the absolute errors of all investigated experiments can be seen in Fig. 8. The comparison between the current 1D with the 2D and 3D simulations indicate comparable predictions to the best solution. It is also the least time consuming model (almost negligible).

One of the most observed findings in Fig. 8 is that although the 3D result was more complicated and suited well with the real experimental set-up, it presented

Table 4 Computational settings for the 2D and 3D CFD simulations

Total bed height	500 mm (2D) 300 mm (3D)
Bed diameter	147 mm
Initial bed height	110 mm
Initial bed voidage	0.45
Under-relaxation factor (pressure, momentum, volume fraction)	0.2
Convergence criteria (continuity, momentum)	1e-5 sec
Computational time step (adaptive)	1e-5 – 3.5e-3 (2D) 1e-4 – 3.5e-3 (3D)
Maximum iteration / time step	200
Total computational time	15 s

somewhat less accurate predictions compared to the 2D and 1D models as shown on subfigure N1.

The comparison between the present 1D, and both the 2D and 3D models on the basis of an overall error and the total computational time for a given system shown in Fig. 8. This figure demonstrates the feasibility of the proposed semi-empirical 1D model in the prediction of axial jetsam concentration in binary fluidized beds. The present 1D model of negligible computation time can give comparable results to the complex 2D and 3D models requiring high computational units. Besides accuracy, also computational efficiency is a very important characteristics of a model in several applications like real-time simulations, operator training, and in advanced control algorithms [44].

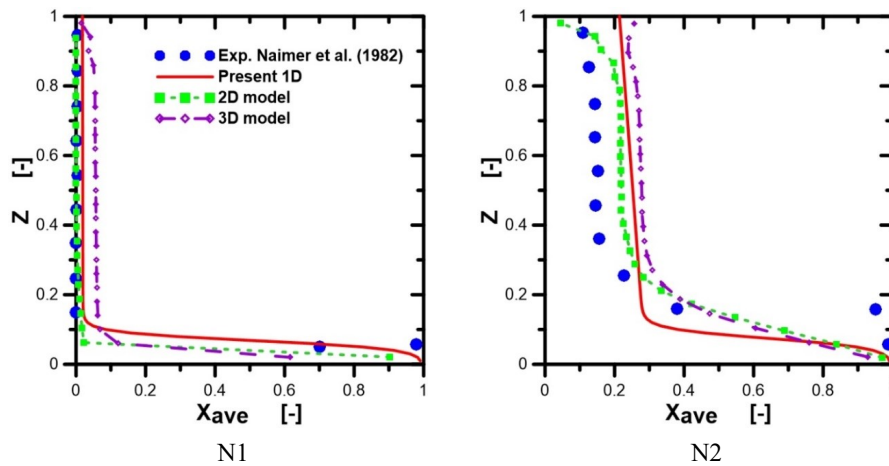


Fig. 7 Comparison between the measured data points (blue symbols), the prediction of the current 1D model (red solid line), and 2D and 3D models (broken lines). (The subfigure captions refer to the experiment IDs in column A of Table 1.)

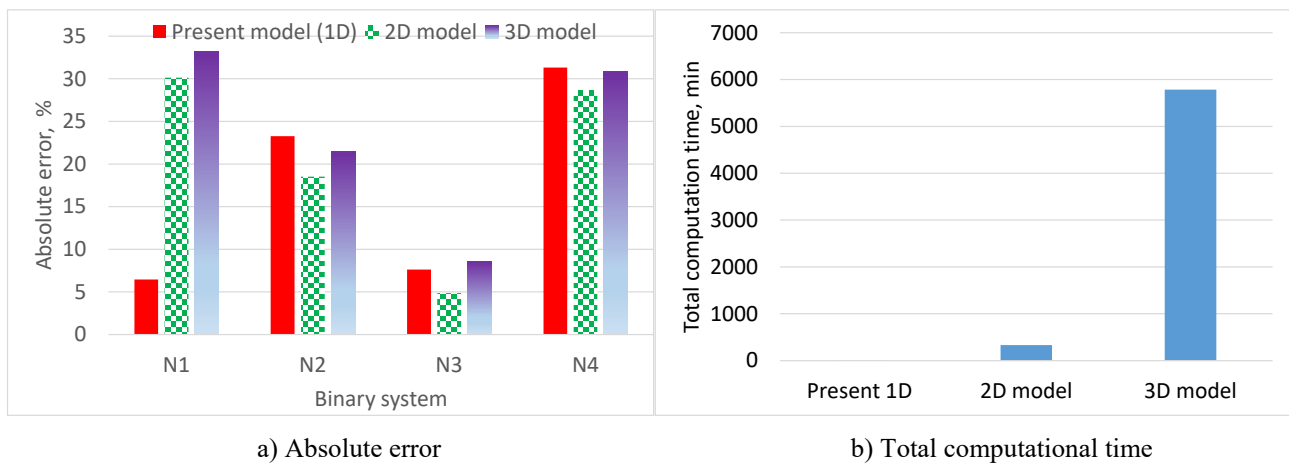


Fig. 8 a) Comparison summary of the errors of the present model (filled red bars), and 2D and 3D models (patterned bars of other colors). (The experiment identifiers below the horizontal axis refer to column A in Table 1.)
 b) Total computation time required by the present 1D model, and the advanced 2D and 3D calculations.

4 Conclusion

In the present research, a semi-empirical 1D model was developed to predict the jetsam axial concentration in binary fluidized beds. The model is based on an available theoretical model, the G–R model, the parameters of which were determined by a compound fitting procedure to published measurements. As a result of this procedure, this model is an overall one, hence its parameters are formulated as functions of the direct operating parameters of the actual fluidized bed system like fluidization velocity, particle densities, etc. The resulting model was compared to all available 1D models on the basis of very versatile parameters and situations ranging from marked segregation to marked mixing. The comparison results show that the accuracy of the present model is better in most cases than that of the previous models, in spite of their being no overall models, but valid ones for specific cases only. The present model was also compared to 2D and 3D simulations, which are available nowadays as high performance commercial hardware and software tools. It became evident that the accuracy of the present 1D model is comparable with those of the 2D and 3D simulations. However, the later codes are numerically much more expensive compared to the present 1D model, which is, therefore, capable for numerous applications like built-in elements of advanced controllers, which run this model inversely, real-time, or as part of an optimum-seeking iteration cycle.

References

- [1] Yates, J. G., Lettieri, P. "Fluidized-Bed Reactors: Processes and Operating Conditions", 1st ed., Springer, 2016.
- [2] Scala, F. (ed.) "Fluidized Bed Technologies for Near-Zero Emission Combustion and Gasification", 1st ed., Woodhead Publishing, Philadelphia, Pennsylvania, USA, 2013.
- [3] Nienow, A. W., Rowe, P. N., Cheung, L. Y.-L. "A quantitative analysis of the mixing of two segregating powders of different density in a gas-fluidised bed", Powder Technology, 20(1), pp. 89–97, 1978.
[https://doi.org/10.1016/0032-5910\(78\)80013-8](https://doi.org/10.1016/0032-5910(78)80013-8)
- [4] Formisani, B., Girimonte, R., Longo, T. "The fluidization pattern of density-segregating binary mixtures", Chemical Engineering Research and Design, 86(4), pp. 344–348, 2008.
<https://doi.org/10.1016/j.cherd.2007.11.004>
- [5] Hoffmann, A. C., Romp, E. J. "Segregation in a fluidised powder of a continuous size distribution", Powder Technology, 66(2), pp. 119–126, 1991.
[https://doi.org/10.1016/0032-5910\(91\)80093-X](https://doi.org/10.1016/0032-5910(91)80093-X)

Nomenclature

C	jetsam concentration	–
d	diameter (of jetsam or flotsam particles)	m
f_w	volumetric fraction of solids in the wake phase	–
u	linear velocity	m/s
X	local jetsam mass fraction in the mixture	–
x_j	total jetsam mass fraction in the mixture	–
Z	dimensionless vertical position in the bed	–
β	axial mixing / segregation parameter	–
γ	phase exchange / circulation parameter	–
λ	exchange / circulation parameter	–
ρ	density (of jetsam or flotsam particles)	kg/m ³
ρ	bulk density	kg/m ³

Subscripts

ave	Average
B	in the bulk phase; big
f	Flotsam
g	Gas
j	Jetsam
mf	minimum fluidization
s	solids, small
W	in the wake phase

Acknowledgement

This work was supported by the National Research, Development and Innovation Fund of Hungary in the frame of FIEK_16-1-2016-0007 (Higher Education and Industrial Cooperation Center) project.

- [6] Jang, H. T., Park, T. S., Cha, W. S. "Mixing–segregation phenomena of binary system in a fluidized bed", Journal of Industrial and Engineering Chemistry, 16(3), pp. 390–394, 2010.
<https://doi.org/10.1016/j.jiec.2009.10.003>
- [7] Palappan, K. G., Sai, P. S. T. "Studies on segregation of binary mixture of solids in continuous fast fluidized bed: Part III. Quantification of performance of the segregator", Chemical Engineering Journal, 145(1), pp. 100–111, 2008.
<https://doi.org/10.1016/j.cej.2008.07.041>
- [8] Peeler, J. P. K., Huang, J. R. "Segregation of wide size range particle mixtures in fluidized beds", Chemical Engineering Science, 44(5), pp. 1113–1119, 1989.
[https://doi.org/10.1016/0009-2509\(89\)87010-1](https://doi.org/10.1016/0009-2509(89)87010-1)
- [9] Formisani, B., Girimonte, R., Longo, T. "The fluidization process of binary mixtures of solids: Development of the approach based on the fluidization velocity interval", Powder Technology, 185(2), pp. 97–108, 2008.
<https://doi.org/10.1016/j.powtec.2007.10.003>

- [10] García-Ochoa, F., Romero, A., Villar, J. C., Bello, A. "A study of segregation in a gas-solid fluidized bed: Particles of different density", *Powder Technology*, 58(3), pp. 169–174, 1989.
[https://doi.org/10.1016/0032-5910\(89\)80111-1](https://doi.org/10.1016/0032-5910(89)80111-1)
- [11] Hartholt, G. P. "Particle Mixing in Gas-Solid Fluidised Beds", PhD Thesis, University of Groningen, 1996.
- [12] Hoffmann, A. C., Janssen, L. P. B. M., Prins, J. "Particle segregation in fluidised binary mixtures", *Chemical Engineering Science*, 48(9), pp. 1583–1592, 1993.
[https://doi.org/10.1016/0009-2509\(93\)80118-A](https://doi.org/10.1016/0009-2509(93)80118-A)
- [13] Leaper, M. C., King, A. C., Burbidge, A. S. "Total Solution of the Gibilaro and Rowe Model for a Segregating Fluidized Bed", *Chemical Engineering & Technology*, 30(2), pp. 161–167, 2007.
<https://doi.org/10.1002/ceat.200600139>
- [14] Tannous, K. (ed.) "Innovative Solutions in Fluid-Particle Systems and Renewable Energy Management", IGI Global, Hershey, Pennsylvania, USA, 2015.
<https://doi.org/10.4018/978-1-4666-8711-0>
- [15] Saidi, M., Basirat Tabrizi, H., Chaichi, S., Dehghani, M. "Pulsating flow effect on the segregation of binary particles in a gas–solid fluidized bed", *Powder Technology*, 264, pp. 570–576, 2014.
<https://doi.org/10.1016/j.powtec.2014.06.003>
- [16] Cano-Pleite, E., Hernández-Jiménez, F., Acosta-Iborra, A., Tsuji, T., Muller, C. R. "Segregation of equal-sized particles of different densities in a vertically vibrated fluidized bed", *Powder Technology*, 316, pp. 101–110, 2017.
<https://doi.org/10.1016/j.powtec.2017.01.007>
- [17] Rüdüsüli, M., Schildhauer, T. J., Biollaz, S. M. A., van Ommen, J. R. "Scale-up of bubbling fluidized bed reactors — A review", *Powder Technology*, 217, pp. 21–38, 2012.
<https://doi.org/10.1016/j.powtec.2011.10.004>
- [18] Geng, S., Jia, Z., Zhan, J., Liu, X., Xu, G. "CFD modeling the hydrodynamics of binary particle mixture in pseudo-2D bubbling fluidized bed: Effect of model parameters", *Powder Technology*, 302, pp. 384–395, 2016.
<https://doi.org/10.1016/j.powtec.2016.09.001>
- [19] Cello, F., Di Renzo, A., Di Maio, F. P. "A semi-empirical model for the drag force and fluid–particle interaction in polydisperse suspensions", *Chemical Engineering Science*, 65(10), pp. 3128–3139, 2010.
<https://doi.org/10.1016/j.ces.2010.02.006>
- [20] Mazzei, L., Lettieri, P. "A drag force closure for uniformly dispersed fluidized suspensions", *Chemical Engineering Science*, 62(22), pp. 6129–6142, 2007.
<https://doi.org/10.1016/j.ces.2007.06.028>
- [21] Gao, X., Wu, C., Cheng, Y., Wang, L., Li, X. "Experimental and numerical investigation of solid behavior in a gas–solid turbulent fluidized bed", *Powder Technology*, 228, pp. 1–13, 2012.
<https://doi.org/10.1016/j.powtec.2012.04.025>
- [22] Luo, K., Wang, S., Yang, S., Hu, C., Fan, J. "Computational Fluid Dynamics–Discrete Element Method Investigation of Pressure Signals and Solid Back-Mixing in a Full-Loop Circulating Fluidized Bed", *Industrial & Engineering Chemistry Research*, 56(3), pp. 799–813, 2017.
<https://doi.org/10.1021/acs.iecr.6b04047>
- [23] Ayeni, O. O., Wu, C. L., Nandakumar, K., Joshi, J. B. "Development and validation of a new drag law using mechanical energy balance approach for DEM–CFD simulation of gas–solid fluidized bed", *Chemical Engineering Journal*, 302, pp. 395–405, 2016.
<https://doi.org/10.1016/j.cej.2016.05.056>
- [24] Toomey, R. D., Johnstone, H. F. "Gaseous Fluidization of Solid Particles", *Chemical Engineering Progress*, 48, pp. 220–226, 1952.
- [25] Gibilaro, L. G., Rowe, P. N. "A model for a segregating gas fluidized bed", *Chemical Engineering Science*, 29(6), pp. 1403–1412, 1974.
[https://doi.org/10.1016/0009-2509\(74\)80164-8](https://doi.org/10.1016/0009-2509(74)80164-8)
- [26] Al-Agha, M. S., Szentannai, P. "1D numerical model for prediction of jetsam concentration in segregating fluidized beds", *Thermal Science*, 2018.
<https://doi.org/10.2298/TSCI170418066A>
- [27] Naimer, N. S., Chiba, T., Nienow, A. W. "Parameter estimation for a solids mixing|segregation model for gas fluidised beds", *Chemical Engineering Science*, 37(7), pp. 1047–1057, 1982.
[https://doi.org/10.1016/0009-2509\(82\)80135-8](https://doi.org/10.1016/0009-2509(82)80135-8)
- [28] Fan, L. T., Chang, Y. "Mixing of large particles in two-dimensional gas fluidized beds", *The Canadian Journal of Chemical Engineering*, 57(1), pp. 88–97, 1979.
<https://doi.org/10.1002/cjce.5450570114>
- [29] Abanades, J. C., Kelly, S., Reed, G. P. "A mathematical model for segregation of limestone-coal mixtures in slugging fluidised beds", *Chemical Engineering Science*, 49(23), pp. 3943–3953, 1994.
[https://doi.org/10.1016/0009-2509\(94\)00209-6](https://doi.org/10.1016/0009-2509(94)00209-6)
- [30] Joseph, G. G., Leboreiro, J., Hrenya, C. M., Stevens, A. R. "Experimental segregation profiles in bubbling gas-fluidized beds", *AIChE Journal*, 53(11), pp. 2804–2813, 2007.
<https://doi.org/10.1002/aic.11282>
- [31] Nakamura, S. "Applied Numerical Methods with Software", Prentice Hall, Englewood Cliffs, New Jersey, USA, 1991.
- [32] Davidson, J. F., Keairns, D. L. (eds.) "Fluidization: Proceedings of the Second Engineering Foundation Conference, Trinity College, Cambridge, England 2-6 April 1978", Cambridge University Press, Cambridge, New York, 1978.
- [33] Tanimoto, H., Chiba, S., Chiba, T., Kobayashi, H. "Jetsam descent induced by a single bubble passage in three-dimensional gas-fluidized beds", *Journal of Chemical Engineering of Japan*, 14(4), pp. 273–276, 1981.
<https://doi.org/10.1252/jcej.14.273>
- [34] Chao, Z., Wang, Y., Jakobsen, J. P., Fernandino, M., Jakobsen, H. A. "Multi-fluid modeling of density segregation in a dense binary fluidized bed", *Particuology*, 10(1), pp. 62–71, 2012.
<https://doi.org/10.1016/j.partic.2011.10.001>
- [35] Zhao, P., Zhu, R., Zhao, Y., Luo, Z. "De-mixing characteristics of fine coal in an air dense medium fluidized bed", *Chemical Engineering Research and Design*, 110, pp. 12–19, 2016.
<https://doi.org/10.1016/j.chemd.2016.03.026>
- [36] Potter, M. C., Wiggert, D. C., Ramadan, B. "Mechanics of fluids", 5th ed., Cengage Learning, Melbourne, Australia, 2017.

- [37] Sahoo, A., Roy, G. K. "Mixing characteristic of homogeneous binary mixture of regular particles in a gas–solid fluidized bed", *Powder Technology*, 159(3), pp. 150–154, 2005.
<https://doi.org/10.1016/j.powtec.2005.08.010>
- [38] Huilin, L., Yunhua, Z., Ding, J., Gidaspow, D., Wei, L. "Investigation of mixing / segregation of mixture particles in gas–solid fluidized beds", *Chemical Engineering Science*, 62(1–2), pp. 301–317, 2007.
<https://doi.org/10.1016/j.ces.2006.08.031>
- [39] Luna, C. M. R., Carrocci, L. R., Arce, G. L. A. F., Ávila, I. "A comparative assessment of empirical and lattice Boltzmann method-based drag models for simulation of gas–solid flow hydrodynamics in a bubbling fluidized bed", *Particuology*, 33, pp. 129–137, 2017.
<https://doi.org/10.1016/j.partic.2016.08.008>
- [40] Mazzei, L., Casillo, A., Lettieri, P., Salatino, P. "CFD simulations of segregating fluidized bidisperse mixtures of particles differing in size", *Chemical Engineering Journal*, 156(2), pp. 432–445, 2010.
<https://doi.org/10.1016/j.cej.2009.11.003>
- [41] ANSYS, Inc. "ANSYS Fluent Theory Guide", SAS IP Inc., USA, 2016.
- [42] Gidaspow, D. "Multiphase Flow and Fluidization: Continuum and Kinetic Theory Descriptions", 1st ed., Academic Press, Boston, Massachusetts, USA, 1994.
- [43] Syamlal, M. "The particle-particle drag term in a multi-particle model of fluidization", EG & G Washington Analytical Services Center, Inc., Morgantown, West Virginia, USA, 1987.
- [44] Szentannai, P. "Power Plant Applications of Advanced Control Techniques", 1st ed., ProcessEng Engineering GmbH, Vienna, Austria, 2010.